

Catalysis Science & Technology

Accepted Manuscript



This is an *Accepted Manuscript*, which has been through the Royal Society of Chemistry peer review process and has been accepted for publication.

Accepted Manuscripts are published online shortly after acceptance, before technical editing, formatting and proof reading. Using this free service, authors can make their results available to the community, in citable form, before we publish the edited article. We will replace this *Accepted Manuscript* with the edited and formatted *Advance Article* as soon as it is available.

You can find more information about *Accepted Manuscripts* in the [Information for Authors](#).

Please note that technical editing may introduce minor changes to the text and/or graphics, which may alter content. The journal's standard [Terms & Conditions](#) and the [Ethical guidelines](#) still apply. In no event shall the Royal Society of Chemistry be held responsible for any errors or omissions in this *Accepted Manuscript* or any consequences arising from the use of any information it contains.



www.rsc.org/catalysis

Bottom-up Approach to Engineer Two Covalent-Porphyrinic Frameworks as Effective Catalyst for Selective Oxidation

Cite this: DOI: 10.1039/x0xx00000x

Received 00th January 2012,
Accepted 00th January 2012

Weijie Zhang,^a Pingping Jiang^{a*}, Ying Wang,^a Jian Zhang,^b and Pingbo Zhang^a

DOI: 10.1039/x0xx00000x

www.rsc.org/

Two kinds of novel functional covalent-organic frameworks were assembled with the porphyrin building and terephthalaldehyde or squaric acid *via* bottom-up approach, respectively. Here, our reported covalent-porphyrinic frameworks with coordinated manganese (III) ions (Mn-CPF-1 and Mn-CPF-2) present promising catalytic property for the selective oxidation of olefins.

Activation of unsaturated bonds is a field of increasing interest in relation to the design of highly active catalysts for selective oxidation reactions. Among them, synthetic metalloporphyrin has been long known as an effective catalyst for oxidation reactions, due to its excellent catalytic performance and high product selectivity.¹ However, the application of metalloporphyrin as catalyst in solution is particularly difficult to achieve because of the formation of catalytically inactive dimers and fast degradation in homogeneous catalysis.² Therefore, it is of great significance to circumvent these challenges.

Covalent-organic framework (COF) is a novel class of porous crystalline organic materials assembled from molecular building blocks by linking light elements (e.g. B, C, N, O) via covalent bond formation (boronic acid trimerization, boronate ester formation, the Schiff base reaction, hydrazone and squaraine linkage) in a periodic manner.³ In terms of catalytic application, COFs have been successfully projected to bridge the gap between heterogeneous materials and homogeneous catalysis.⁴ Currently, porphyrins and metalloporphyrins afford ideal synthons for building blocks in the construction of covalent porphyrinic networks in analogy to robust inorganic zeolites for versatile application.⁵

To be more precise, the covalent-porphyrinic frameworks (CPFs) with accessibility of the open channels, can be considered as self-supported catalysts with an enhanced performance due to their high-density active sites into frameworks. The tetrapyrrolic macrocycles of porphyrins play an important role in the design of extended supramolecular lattices, which derives from their robust structure, remarkable thermal and oxidative stability, and unique catalytic properties. In addition, the heterogeneous nature of CPFs

can be very useful to separate the catalyst from the products of interest, recover it after simple filtration procedures and finally regenerate it for successive catalytic runs. Therefore, it may be a valuable trial to target efficient heterogeneous catalysts with open coordination frameworks *via* bottom-up strategy, which is essential to catalysis application. Here, the bottom-up method enables direct visualization of structure and makes it possible to get a detailed insight into the relationship between the structure and the catalytic activity by structural interrogation.

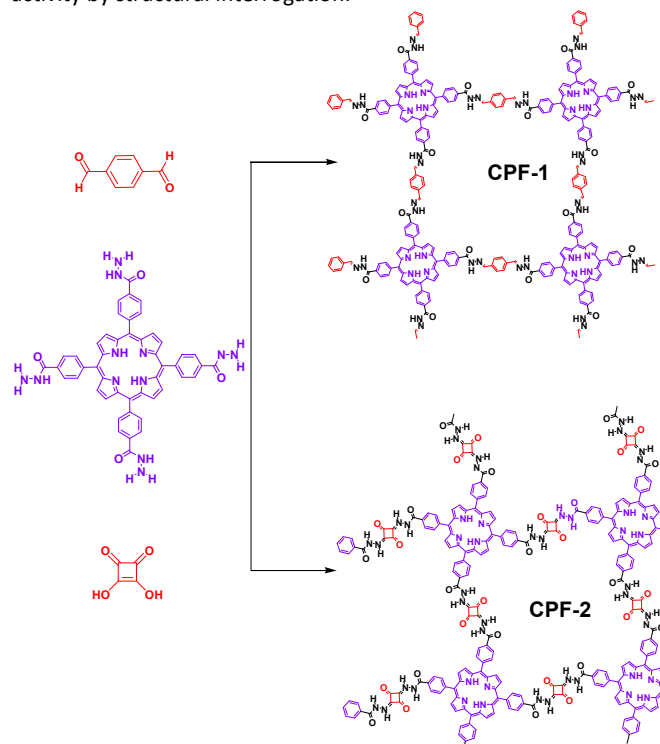


Fig. 1. Schematic representation of molecular building blocks of CPF-1 and CPF-2

With this background in mind, we reported the development of new CPFs based on the hydrazone and squaraine linkage (Fig. 1). It has been previously studied that condensation of hydrazide with aldehyde⁶ or squaraine⁷ was a thermodynamically controlled reaction. During this reaction, the formation of hydrazone or squaraine derivatives and water by-products was proceeded. Accordingly, we employed meso-Tetra (4-hydrazidocarbonylphenyl)porphyrin (Scheme 1, THCPP) with four hydrazide groups at periphery as the aldehyde or squaraine component to condense with hydrazine, with the aim to demonstrate the feasibility of the strategy and features of a new class of CPFs. Furthermore, the crystal data of THCPP (Fig. S1) obtained by a solvent diffusion method, substantiated this point that the macrocycles of porphyrin units could be classified as 2D-C₄ blocks^{3c} on a simplified symmetry notation with a rigid nature and discrete bonding direction of arenes, in order to make aromatic π systems.

All CPFs were synthesized by solvothermal reactions (See the Supporting Information). In order to introduce catalytically active sites into monomers, a metal-porphyrin complexation was employed. As expected, the resultant Mn-HTCPP showed characteristic peaks as $m/z=899$, in the MALDI-MS spectra (Fig. S3). CPF-1 and CPF-2 were given as purple solids in 60% and 55% isolated yields. Mn-CPF-1 and Mn-CPF-2 were obtained as green powder in 52% and 46% yields. As shown in Fig. S4 and S5, the FT-IR spectra of CPF-1 and Mn-CPF-1 showed stretching modes at 1660 cm^{-1} that are characteristic of C=N moieties. For CPF-2 and Mn-CPF-2, the FT-IR exhibited a vibration band at 1521 cm^{-1} , characteristic of a C=O band from squaraine (SQ).

The crystalline structure of the synthesized CPF materials was resolved by the XRD measurements in conjunction with structural simulation. Atomic positions and cell sizes of modelled COF layers were optimized using Material studio software. XRD studies on CPF-1 and CPF-2 in Fig. 6 and Fig. 7 indicated certain accordance between experimental patterns and the simulated patterns based on the modelled structure. Although the intensities of XRD pattern for CPF-1 and CPF-2 were poor, the experimental XRD pattern of CPF-1 and CPF-2 also partly matched well with the simulated pattern of the AB stacking model in Fig. S6 and S7, relative to AA stacking model. Obviously, it was still not yet clear for other diffraction peaks ($40^\circ > 2\theta > 15^\circ$) in CPFs. The cross-linking of CPFs may give rise to uncertain conformation. Nevertheless, Mn-CPF-1 and Mn-CPF-2 did not reveal any obvious diffraction peaks at same solvothermal growth condition, implying that they were composed of an amorphous network. This was probably due to the different solution between porphyrins and metalloporphyrins. Compound CPF-1 and CPF-2 both exhibited a typical type III isotherm with a surface area of 158 m^2/g for CPF-1 and 92 m^2/g for CPF-2, respectively (Fig. S8). The prepared COFs showed N₂ adsorption isotherms with low surface areas. It can be speculated that these COFs adopt a thin layer morphology. Due to the thin-layered structures, long-rang pore formation is hindered, rendering N₂ adsorption possible only in the shallowest, most accessible pores.⁸ Alternatively, it may be helpful to prepare the crystalline CPF-1 or 2 first, subsequently introduce Mn to get Mn-catalyst with crystalline structure. These studies will be reported separately in the near future.

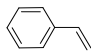
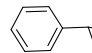
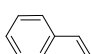
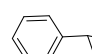
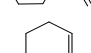
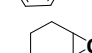
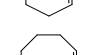
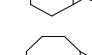
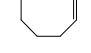
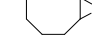
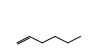
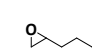
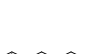

FE-SEM revealed that CPF-1 and CPF-2 were composed of uniform micrometre-scale bet morphology of dimension ca. 200nm and larger particle of ca. 0.5-1 μm , respectively (Fig. S9). Both samples were stable in various solvents. TGA of the activated CPF-1

and Mn-CPF-1 had no obvious weight loss until 350 $^\circ\text{C}$ (Fig. S10). One may notice that the frameworks of CPF-2 and Mn-CPF-2 started to decompose around 230 $^\circ\text{C}$, which can be attributed to a weak thermal stability of squaraine linkage (Fig. S11).

The inductively coupled plasma atomic mass spectrometry analysis (ICP-MS) results showed that the density of active Mn sites reached as high as 1.7 mmol/g for Mn-CPF-1 and 1.6 mmol/g for Mn-CPF-2, respectively. The Mn content of Mn-CPF was found to be more than 10 times higher than ever reported amount of Mn complex grafted on insoluble materials, like mesoporous sieve.⁹ In this regard, the bottom-up strategy could facilitate metalloporphyrin catalyst with a high active sited density, owing to their accessibility, facile derivatization and ability to bind a wide variety of metal ions, like Cu and Fe ions.

A recent research also showed that framework catalysts with AB stacked 3D net, constructed by Mn-porphyrin as bridging linker and Zn as node, provided accessibility for the Mn(III) active site to molecular substrate and accordingly exhibited excellent catalytic properties.¹⁰ Thus, we were encouraged to demonstrate catalytic efficiency of metallic CPF materials. First of all, styrene was employed to investigate their different catalytic performance. Although the conversion of styrene was very high, 68 % of selectivity for Mn-CPF-1 and 60 % for Mn-CPF-2 exhibited after 24h (Table 1, entry 1-2). Mn-CPF-1 led to a faster reaction rate, compared to Mn-CPF-2 shown in Fig. S12. The comparably low selectivity of styrene epoxides was related with the low electron density of styrene which usually reduced their nucleophilicity toward electrophilic oxygen of porphyrin-Mn(V)=O.

Table 1. Scope of Mn-CPF catalysed epoxidation of alkenes.^[a]

Entry	Substrate	Product	Catalyst	Conversion (%) ^[b]	Selectivity (%) ^[c]
1			Mn-CPF-1	99/96 ^[d]	68/62 ^[e]
2			Mn-CPF-2	93	60
3			Mn-CPF-1	99	>99
4			Mn-CPF-1	95	>99
5			Mn-CPF-1	81	>99
6			Mn-CPF-1	66	>99
7			Mn-CPF-1	20	>99

[a] Olefin (1.0 mmol), TBHP (1.5 mmol), catalyst (0.01 mmol), acetonitrile (3.0 mL) and bromobenzene (50 mg) sealed as internal standard in a Teflon-lined screwcap vial were stirred at 80 $^\circ\text{C}$ for 24 h. [b] Conversion [%] and [c] selectivity [%] were determined by GC using an SE-54 column (50 $^\circ\text{C}$ for 1 min, then 10 $^\circ\text{C min}^{-1}$ up to 140 $^\circ\text{C}$ and 140 $^\circ\text{C}$ for 15 min). [d] After third cycles. [e] The by-products were benzaldehyde and benzenacetaldehyde.

The excellent heterogeneous catalysts should not only have high catalytic activity and selectivity, but should also be structurally stable and thus be easily recovered for continuous usage. Compound Mn-CPF-1 can be simply recycled by filtration, which was subsequently reused in successive runs (Figure S13). Although the reaction rate decreased, the recycled Mn-CPF-1 still exhibited a very high conversion of 96 % and selectivity of 62 % when styrene

being used as substrate, thus indicating that Mn-CPF-1 was indeed a heterogeneous catalyst for styrene epoxidation (Table 1, entry 1).

The catalytic activity of the epoxidation of cyclohexene and cyclooctene with different steric sizes was further investigated at same condition (Table 1, entry 3 and 4). Obviously, Mn-CPF-1 exhibited a high catalytic activity and selectivity for epoxidation of cyclohexene. However, cyclooctene with a larger steric size led to a reduced conversion, which suggested that the active catalytic sites should be the Mn-porphyrin moieties within the pores of Mn-CPF-1. In order to further understand the steric effect on catalytic efficiency, a range of natural alkenes were selected to be oxidized in this catalytic system. Increasing the length of linear alkenes triggered lower epoxide yield due to their different steric size of substrates (Table 1, entry 5-7).

To confirm the aforementioned claim, we compared the catalytic activities of Mn-CPF-1 with their molecular components of MnCl₂ and Mn-HTCPP under identical reaction conditions. Mn-HTCPP did show quite moderate catalytic activity that could transform 79 % of the cyclohexene into the cyclohexene oxide (Table 2, entry 2), but still were not as efficient as heterogeneous Mn-CPF-1 (99 % conversion). MnCl₂ showed a lower catalytic activity with conversions of 35 % (Table 2, entry 3). No increase of trace product was detected after the filtrate from a mixture of Mn-CPF-1 in acetonitrile (Table 2, entry 4). Low epoxide yield was also obtained when no catalytic active sites were added (Table 2, entry 5 and 6). The different catalytic stabilities of Mn-CPF-1 and Mn-HTCPP in the catalytic epoxidation of olefins can be attributed to the homogeneous metalloporphyrins catalyst having very high suicidal inactivation by formation of the catalytically inactive u-oxometalloporphyrin dimers,¹¹ whereas integration of metalloporphyrins within the pore surfaces of Mn-CPF-1 can significantly enhance and sustain the catalytic activities by blocking formation of the inactive species.

Table 2. Scope of catalysed epoxidation of cyclohexene^[a]

Entry	Catalyst	Conversion (%) ^[b]	Selectivity (%) ^[c]
1	Mn-CPF-1	99	>99
2	Mn-HTCPP	79	53
3	MnCl ₂	35	78
4	filtrate ^[d]	20	4
5	blank	19	5
6	CPF	32	7

[a] Olefin (1.0 mmol), TBHP (1.5 mmol), catalyst (0.01 mmol), acetonitrile (3.0 mL) and bromobenzene (50 mg) as internal standard sealed in a Teflon-lined screwcap vial were stirred at 80 °C for 24 h. [b] Conversion [%] and [c] selectivity [%] were determined by GC using an SE-54 column. [d] After catalytic assay for Mn-CPF-1.

Although Mn-CPF-1 showed a superior catalytic efficiency to Mn-CPF-2, the nature of Mn sites in Mn-CPFs has not been revealed. To identify this point, XPS analysis can help to reveal the oxidant

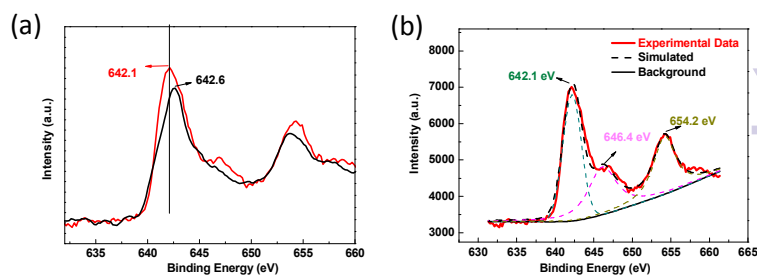


Fig. 2. (a) XPS spectra for the clean Mn-CPF-1 surface, fresh catalyst (black line) and Mn-CPF-1 (red line) and (b) XPS spectra for Mn-CPF-2, Mn 2p_{3/2} and high valent-oxo region.

state of Mn sites of molecules in Mn-CPFs. As shown in Fig. 2, one may notice that the peak value of Mn2p_{3/2} in Mn-CPF-1 shifted to a higher value of 642.6 eV, with respect to the value of 642.1 eV in Mn-CPF-1 and 642.2 eV in the previous research¹². In this case, the redox property of the Mn complexes in Mn-CPF-1 was greatly influenced after being assembled into extended π systems, that is, the charge was positively transferred from Mn (III) centre to linkage. There was a desirable catalysis-promoted electronic environment around of Mn (III) center in Mn-CPF-1. Therefore, Mn-CPF-1 urged a more efficient catalysis than Mn-CPF-2, which was consistent with the catalytic data. As Mn-CPF-2 for example, there was a satellite peak at 646.4 and 654.2 eV, respectively, beside the main peak of Mn2p_{3/2}. The resulting satellite peak may be attributed to the manganese-oxo species from the surface of catalyst.

In summary, we successfully constructed two kinds of covalent-porphyrinic framework based on the crystal structure of HTCPP *via* bottom-up approach, namely CPF-1 with a hydrazone linkage and CPF-2 linked by the squaraine linkage. After incorporating catalytic Mn (III) centre into monomers, the catalytic activity was carefully examined. The results showed that Mn-CPF-1 was the most effective among those tested involving homogenous and heterogeneous system. Of further importance, a detailed XPS study evidenced that Mn-CPF-1 owned a more desirable electronic environment than Mn-CPF-2. This could help to further understand the relationship between material structure and catalytic activity.

Special thanks to Dr. Liu from East China University of Science and Technology for his help on test of XPS data. This work was supported financially by the National "Twelfth Five-Year" Plan for Science & Technology (2012BAD32B03), the National Natural Science Foundation of China (20903048) and the Innovation Foundation in Jiangsu Province of China (BY2013015-10).

Notes and references

^a The Key Laboratory of Food Colloids and Biotechnology, School of Chemical and Material Engineering, Jiangnan University, Wuxi 214122, P.R. China. E-mail: ppjiang@jiangnan.edu.cn

^b School of Chemistry and Environmental Science, Lanzhou City University, Lanzhou 730000, P.R. China

Electronic Supplementary Information (ESI) available: [HNMR, FT-IR, PXRD, TG analysis, crystal data and catalytic details]. See DOI: 10.1039/c000000x/

1 (a) P. R. Ortiz de Montellano, *Chem. Rev.*, 2010, **110**, 932; (b) M. Costas, *Coord. Chem. Rev.*, 2011, **255**, 2912.

2 T. C. Bruice, *Acc. Chem. Res.*, 1991, **24**, 243.

3 (a) A. P. Cote, A. I. Benin, N. W. Ockwig, M. O'Keeffe, A. J. Matzger and O. M. Yaghi, *Sci.*, 2005, **310**, 1166; (b) S. Y. Ding and W. Wang, *Chem. Soc.*

- Rev., 2013, **42**, 548; (c) X. Feng, X. Ding and D. Jiang, *Chem. Soc. Rev.*, 2012, **41**, 6010.
- 4 (a) L. Li, Z. Chen, H. Zhong and R. Wang, *Chem. Eur. J.*, 2014, **20**, 3050; (b) X. Chen, N. Huang, J. Gao, H. Xu, F. Xu and D. Jiang, *Chem. Commun.*, 2014, **50**, 6161; (c) X. Feng, L. Chen, Y. Dong and D. Jiang, *Chem. Commun.*, 2011, **47**, 1979.
- 5 (a) Z. Xiang, Y. Xue, D. Cao, L. Huang, J. F. Chen and L. Dai, *Angew. Chem. Int. Ed.*, 2014, **53**, 2433; (b) X.-S. Wang, M. Chrzanowski, D. Yuan, B. S. Sweeting and S. Ma, *Chem. Mater.*, 2014, **26**, 1639; (c) V. S. P. K. Neti, X. F. Wu, S. G. Deng and L. Echegoyen, *Polym. Chem.*, 2013, **4**, 4566; (d) R. K. Totten, Y. S. Kim, M. H. Weston, O. K. Farha, J. T. Hupp and S. T. Nguyen, *J. Am. Chem. Soc.*, 2013, **135**, 11720; (e) S. Wan, F. Gándara, A. Asano, H. Furukawa, A. Saeki, S. K. Dey, L. Liao, M. W. Ambrogio, Y. Y. Botros, X. Duan, S. Seki, J. F. Stoddart and O. M. Yaghi, *Chem. Mater.*, 2011, **23**, 4094; (f) X. M. Liu, H. Li, Y. W. Zhang, B. Xu, A. Sigen, H. Xia and Y. Mu, *Polym. Chem.*, 2013, **4**, 2445.
- 6 (a)F. J. Uribe-Romo, C. J. Doonan, H. Furukawa, K. Oisaki and O. M. Yaghi, *J. Am. Chem. Soc.*, 2011, **133**, 11478; (b)D. N. Bunck and W. R. Dichtel, *J. Am. Chem. Soc.*, 2013, **135**, 14952.
- 7 A. Nagai, X. Chen, X. Feng, X. Ding, Z. Guo and D. Jiang, *Angew. Chem. Int. Ed. Engl.*, 2013, **52**, 3770.
- 8 B. P. Biswal, S. Chandra, S. Kandambeth, B. Lukose, T. Heine and R. Banerjee, *J. Am. Chem. Soc.*, 2013, **135**, 5328.
- 9 (a)G. M. Ucoski, F. S. Nunes, G. DeFreitas-Silva, Y. M. Idemori and S. Nakagaki, *Appl. Catal. A: Gen.*, 2013, **459**, 121; (b)T. Poursaberi, M. Hassanisadi, K. Torkestani and M. Zare, *Chem. Eng. J.*, 2012, **189**, 117; (c) M. Moghadam, S. Tangestaninejad, V. Mirkhani, I. Mohammadpoor-Baltork and M. Moosavifar, *J. Mol. Catal. A: Chem.*, 2009, **302**, 68; (d)D. H. Shen, L. T. Ji, Z. G. Liu, W. B. Sheng and C. C. Guo, *J. Mol. Catal. A: Chem.*, 2013, **379**, 15.
- 10 C. Zou, T. Zhang, M. H. Xie, L. Yan, G. Q. Kong, X. L. Yang, A. Ma and C. D. Wu, *Inorg. Chem.*, 2013, **52**, 3620.
- 11 J. P. Collman, X. Zhang, V. J. Lee, E. S. Uffelman and J. I. Brauman, *Sci.*, 1993, **261**, 1404.
- 12 J. Xie, Y. J. Wang and Y. Wei, *Catal. Commun.*, 2009, **11**, 110.